Symbolic dynamics analysis of chaotic time series with a driven frequency

Zuo-bing Wu
Institute of Theoretical Physics, Academia Sinica, P.O. Box 2735, Beijing 100080, China
(Received 18 April 1995)

A simple method to determine a partition line from chaotic time series with a driven frequency is devised, so that the embedded strange attractor can be divided effectively by the partition line. After the determination of grammatical rules, symbolic dynamics is established from the chaotic time series. The symbolic dynamics provides a global systematics of unstable periodic orbits within the strange attractor. With the global property, the symbolic dynamics is applied to find unstable periodic orbits and predict the chaotic time series with finite accuracy and symbolic sequences with high accuracy.

PACS number(s): 05.45.+b, 47.52.+j

I. INTRODUCTION

Since Lorenz [1] found a strange attractor in a model to simulate the Earth's atmosphere, chaotic motion has been observed in many experiments, for example, the Belousov-Zhabotinskii reaction [2], the CO_2 laser [3], and the NMR oscillator [4]. The reconstruction of strange attractors from chaotic time series [5–7] has by now become a routine procedure. It results from an inverse problem of nonlinear dynamics and is different from the classical stochastic analysis of time series. This method enables us to apply the theory of dynamical systems [8] to analyze chaotic behavior in an experimental system without any prior knowledge on the governing equations or relevant degrees of freedom.

Being a coarse-grained description [9], symbolic dynamics is one of the popular methods used in studying chaotic behavior in low-dimensional dissipative systems. It provides a description of the site of unstable periodic points within strange attractor in a Poincaré section and gives a rigorous way of understanding their global systematics [10,11]. In terms of symbolic sequences that encode the periodic orbits in a one to one correspondence, topological property shared by a universal class of dynamical systems can be studied conveniently. The topological analysis is based on describing the knotted relation of the periodic orbits in phase space [12]. A template can be used to present the global organization of the knotted periodic orbits [13]. Symbolic dynamics includes two main aspects: first, a symbolic description of orbits by dividing the phase space into a number of regions with different symbols; second, an affirmation of the admissibility for each permutation of finite symbols by determining grammatical rules for symbolic sequences.

Recently, the validity of the extended Bloch-type laser (EBL) model for a chaotic NMR laser has been demonstrated by comparing structures of strange attractors and periodic orbits in the delay Poincarè section between the model and the experiment [14]. A binary partition line is determined approximately by distinguishing 15 periodic points up to order 9 in a one to one correspondence. However, this is only a symbolic description of the periodic orbits. The symbolic dynamics for the EBL model has been given in Ref. [15], where a partition line of the z-y plane is determined from the tangencies of forward and backward foliations. The ordering rules and admissibility condition are constructed and the allowance or forbiddance of periodic sequences up to order 9 and not greater than RL^3R^2L in the U sequence is determined. But this method of establishing symbolic dynamics depends on models, and is not effective for chaotic time series.

The method for the determination of a partition line from chaotic time series in Ref. [14] is very complicated. In particular, the partition line is only effective to distinguish finite periodic orbits but not to divide the strange attractor. So, up to now, establishing symbolic dynamics from chaotic time series and applying it to analyze the time series have not been discussed.

This paper addresses the above questions by using chaotic time series from the EBL model and is organized as follows. In Sec. II A we devise a simple method to determine a partition line from the time series, so that the strange attractor is divided effectively by the partition line. In Sec. II B we determine grammatical rules and establish symbolic dynamics from the time series. In Sec. III A we display the global systematics of periodic orbits and apply the symbolic dynamics to find unstable periodic orbits. In Sec. III B we apply the symbolic dynamics to predict the time series and symbolic sequences. Finally, in Sec. IV we offer the summary and conclusion.

II. ESTABLISHING SYMBOLIC DYNAMICS FROM CHAOTIC TIME SERIES

A. Determining a partition line

The EBL model for a chaotic NMR laser in the rotating-frame approximation is described by

$$\begin{aligned} \dot{x} &= \sigma[y - x/(1 + A\cos\omega t)], \\ \dot{y} &= -y(1 + ay) + rx - xz, \\ \dot{z} &= -bz + xy, \end{aligned} \tag{1}$$

where, as given in Ref. [14], the parameters are $\sigma = 4.875$, $A = 0.018$, $\omega = 0.031\,68$, $a = 0.2621$, $r = 1.807$, and $b = 2 \times 10^{-4}$. The equations we used in actual calculation are scaled from Eqs. (1) by setting $(x, y, z, t, \omega) \rightarrow (xx^*, yy^*, zz^*, t/x^*, \omega x^*)$, where $x^* = y^* = [b(r-1)]^{1/2}$, $z^* = r - 1$. We integrate the equations using a fourth-order Runge-Kutta method with a fixed time step of $T/1000$ ($T = 2\pi/\omega$ is a period of the forcing) and pick up a set of initial points in the phase space at time $t_0 = T/10$:

$$\begin{aligned} x_0 &= y_0(1 + A\cos\omega t_0), \\ y_0 &= 1.2 + 0.005i \quad (i = 1, 2, \ldots, 200), \\ z_0 &= 1. \end{aligned} \tag{2}$$

After discarding the first 20 periods to allow each trajectory to fall in strange attractor, we recode chaotic time series $y(t)$ from trajectories of the following 50 periods.

For the periodically driven system, as given in Refs. [14,16], we determine delay time $\tau = T/5$, so that the leafs within the strange attractor in the delay Poincaré section $[y(t), y(t+\tau); \phi]$ for each phase ϕ are nonintersected.

The strange attractor is embedded in an m-dimensional phase space by constructing vectors of the form $\mathbf{X} = \{y(t), y(t+\tau), \ldots, y(t+(m-1)\tau)\}$ from the time series. We first make a choice of the embedding dimension m=6, which is the minimal integer for $m > 2D_1 + 1$, as given in Ref. [14]. The method of close returns [17] with integer multiples of the driven period T is used to locate shadowing unstable periodic orbits. When an initial phase ϕ is chosen to be $T/10$, the cycles up to order 8 with symbolic sequences not greater than RLR in the U sequence are found. Since the requirement of embedding dimension in the theorem [6,7] is only a sufficient condition for the embedding of an attractor, the embedology can be applied in the phase space whose dimension m is less than $2D_1 + 1$. We also find the cycles in the embedding spaces with dimensions 4 and 5.

The stability of each orbit is estimated from a linear approximation of the dynamics at a periodic point using nearby trajectories [18,19]. The nontrivial elements in the Jacobian matrix of the delay Poincaré map with the driven period T are determined by using the methods of singular value decomposition of a matrix and the generalized inverse matrix. From the time evolution operator of the periodic orbit, we can determine eigenvalues and eigenvectors at each periodic point in the delay Poincaré section. For the eigenvalue $\lambda > 1$ (< 1), we plot a short line with the horizontal projection 0.1 (0.05) from the periodic point in the delay Poincaré section along the corresponding unstable (stable) eigenvector direction. All periodic points up to order 8 with two short lines are displayed in Fig. 1. Figure 2 is a blowup of the boxed region in Fig. 1. We can infer a line, that divides the strange attractor in the delay Poincaré section into two parts from the following observation. In the upper (lower) part, which is marked by L (R), the rotation of an acute angle from the unstable eigenvector direction to the stable eigenvector direction is clockwise (counterclockwise). Thus there is a point in each leaf within the strange attractor where the stable and unstable eigenvectors direction are parallel to each other, i.e., the acute angle between the stable and unstable eigenvector directions is zero. Since the stable and unstable eigenvectors display the directions of forward and backward foliations passing through the point, the point is one of the homoclinic tangency points between forward and backward foliations.

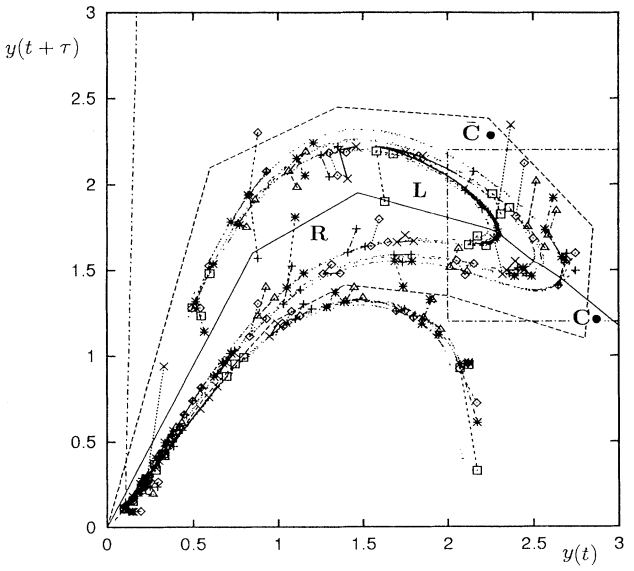

FIG. 1. All points of periodic orbits up to order 8 with their eigenvector directions and strange attractor with the partition lines $C\bullet$ and $\bar{C}\bullet$ in the delay Poincaré section $[y(t), y(t+\tau); T/10]$.

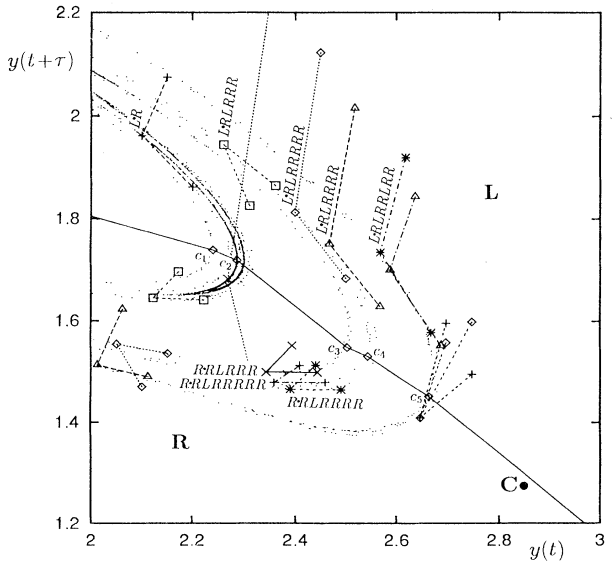

FIG. 2. A blowup of the boxed region in Fig. 1. The five homoclinic tangency points ($c_1 - c_5$) in the partition line $C\bullet$ are labeled by squares.

After having an estimated local region where the tangency point in the leat exists, we can further determine the angle between eigenvector directions at a given point in the region using the forward and backward maps constructed from the time series. It is based, in general, on the convergence of the eigenvector directions at a given point in the limit of long orbit segments and the yield of an invariant direction field for the map [20,21]. We can select a point where the acute angle between stable and unstable eigenvector directions is very small as an approximation to the tangency point. In Fig. 2, five backward foliations have been identified in the strange attractor and a piecewise linear curve passing through the five tangency points approximates a partition line. To divide the strange attractor in the delay Poincaré section for establishing symbolic dynamics, the partition line has higher accuracy than that given in Ref. [14].

So far, we have devised a simple method to determine a partition line from chaotic time series with a driven frequency so that the embedded strange attractor can be divided effectively by the partition line. It is based on the hyperbolic periodic points being in the invariant manifolds and their stable and unstable eigenvectors displaying the stable and unstable manifolds passing through the periodic points.

B. Determining grammatical rules

After the partition line is determined, each point of the delay Poincaré map is encoded by the letter R or L. Thus a point of a chaotic orbit in the delay Poincaré section corresponds to a doubly infinite symbolic sequence composed of the letters R and L, i.e. $S = \cdots s_{-m} \cdots s_{-1} s_0 \bullet s_1 s_2 \cdots s_n \cdots$, where s_n is the code for the nth point of the forward orbit and s_{-m} the code for the mth point of the backward orbit. The present point is indicated by $s_0\bullet$. The solid dot divides the doubly infinite sequence into two semi-infinite sequences, i.e., the backward sequence $\cdots s_{-m} \cdots s_{-1} s_0 \bullet$ and the forward sequence $\bullet s_1 s_2 \cdots s_n \cdots$.

According to the distribution of leafs within the strange attractor that display backward foliations, we can determine the ordering rules. Since the structure of the strange attractor in the delay Poincaré section is similar to that of Hénon map, we introduce the ordering rules of Hénon map with positive and negative values of the determinant of the Jacobian matrix, respectively. They have the same ordering rule for forward sequences, which is described as

$$\bullet ER \cdots > \bullet EL \cdots, \bullet OR \cdots < \bullet OL \cdots, \tag{3}$$

and different ordering rules for backward sequences, which are respectively described as

$$\cdots RE\bullet > \cdots LE\bullet, \cdots RO\bullet < \cdots LO\bullet \tag{4}$$

and

$$\cdots RE'\bullet > \cdots LE'\bullet, \cdots RO'\bullet < \cdots LO'\bullet\,, \tag{5}$$

where the common leading strings E (E') and O (O') consist of letters R and L and contain an even and an odd number of the letter R (L), respectively.

It is convenient to express the ordering rules in terms of a metric representation by real numbers in $[0,1]$. First, we assign an integer $\epsilon_i = 1(-1)$ to a symbol s_i when it is L (R). Then, for the ordering rule (3), we assign to the forward sequence $\bullet s_1 s_2 \cdots s_n \cdots$ a number

$$\alpha = \sum_{i=1}^{\infty} \mu_i 2^{-i}, \tag{6}$$

where

$$\mu_i = \begin{cases} 0 & \text{if } \prod_{j=1}^{i} \epsilon_j = 1, \\ 1 & \text{if } \prod_{j=1}^{i} \epsilon_j = -1. \end{cases}$$

Similarly, for the ordering rule (4) or (5), a number β assigned to the backward sequence $\cdots s_{-m} \cdots s_{-1} s_0 \bullet$ is defined by

$$\beta = \sum_{i=0}^{\infty} \nu_i 2^{-i}, \tag{7}$$

where

$$\nu_i = \begin{cases} 0 & \text{if } \prod_{j=0}^{i} \epsilon_{-j} = 1 \text{ or if } \prod_{j=0}^{i} (-\epsilon_{-j}) = -1, \\ 1 & \text{if } \prod_{j=0}^{i} \epsilon_{-j} = -1 \text{ or if } \prod_{j=0}^{i} (-\epsilon_{-j}) = 1. \end{cases}$$

In this representation a doubly infinite symbolic sequence corresponds to a point in the unit square of the α-β symbolic plane. The forward and backward foliations become vertical and horizontal lines, respectively. A point on the partition line $C\bullet$ may symbolically be represented as $QC \bullet XP$ (X stands for L or R, P or Q stands for a string consisting of R and L). A rectangle enclosed by the lines $QR\bullet$, $QL\bullet$, $\bullet XP$, and $\bullet RL^{\infty}$ forms a forbidden zone in the symbolic plane. Each tangency point on the partition line rules out a rectangle in the symbolic plane. The union of the forbidden rectangles forms the fundamental forbidden zone, whose boundary is the pruning front.

Each approximated tangency point is near an exact one, so there is a difference between the symbolic sequence of the tangency point and that of its corresponding exact one. However, it does not influence the determination of the ordering rules; in other words, the fundamental forbidden zone in the symbolic plane is robust. For the ordered foliations in the delay Poincaré section in Fig. 2, the values of α and β in the upper (lower) region of the fundamental forbidden zone are monotonically changed from the tangency point c_1 to c_5 along the partition line $C\bullet$. According to the ordering rules (3) and (4), and (3) and (5), we draw fundamental forbidden zones in Figs. 3(a) and 3(b), respectively. In Fig.

3(b), from c_1 to c_5 along the partition line $C\bullet$, the value of α is monotonically increased in the upper region of the fundamental forbidden zone, but the value of β is monotonically unchanged. In Fig. 3(a) the values of α and β are monotonically increased in the upper region of the fundamental forbidden zone from c_1 to c_5 along the partition line $C\bullet$. So we take ordering rules (3) and (4) to establish symbolic dynamics.

When the foliations are ordered by using the ordering rules, the geometry of tangencies of the forward and backward foliations places a restriction on the allowance for all permutations of finite symbols. Since the ordering rule for forward sequences is the same as that of the one-dimensional unimodal map, we only need to examine the U sequence. We consider a set of tangencies $\{c_i\}=\{Q_iC\bullet X_iP_i\}$ for $i=1,\ldots,5$. A symbolic sequence $U\bullet V$ with $U\bullet$ between $Q_iR\bullet$ and $Q_iL\bullet$ and at the same time $\bullet V > \bullet X_iP_i$ must be forbidden by the tangency c_i. In the symbolic plane the sequence $U\bullet V$ corresponds to a point inside the forbidden zone of the tangency c_i. If the shift of a sequence $\cdots s_{k-2}s_{k-1}\bullet s_ks_{k+1}\cdots$ satisfies the condition that the backward sequence $\cdots s_{k-2}s_{k-1}\bullet$ is not between $Q_iR\bullet$ and $Q_iL\bullet$ and at the same time $\bullet X_iP_i > \bullet s_ks_{k+1}\cdots$, then this shift is not forbidden by the tangency c_i. Owing to the property of well-ordered foliations, the shift must not be forbidden by any tangencies. Thus we may say that the shift is allowed according to the tangency. A necessary and sufficient condition for a sequence to become an allowed one is that all of its shifts are allowed according to the set of tangencies.

To check the admissibility condition from the set of tangencies, we can draw points representing real sequences generated from the delay Poincaré map in the symbolic plane in Fig. 3(a). The fundamental forbidden zone contains no point of the allowed sequences. It shows that the determined partition line and grammatical rules are effective.

In Fig. 2 the following tangency points are identified on the partition line $C\bullet$, for c_1, c_2, c_3, c_4, and c_5, respectively:

$$\cdots LRRRLRLRLRRRR|RLRRLRC\bullet\ RLRLRLRRRLRLR|LRRRLRR\cdots,$$
$$\cdots RRLRRLRR|RLRLRLRRRLRC\bullet\ RLRRRLRLRLRRRLR|LRLRR\cdots,$$
$$\cdots L|RRRRLRRLRLRRLRLRRRC\bullet\ RLRRRRLRRLRLR|RRRLRLR\cdots,$$
$$\cdots RLRRRRRRRRLR|LRRRRRRC\bullet\ RLRRLRLRRLRRRR|LRRRRL\cdots,$$
$$\cdots RLRRLRLRLRLR|RRLRLRRC\bullet\ RLRRLRRLRLR|LRLRLRRRL\cdots,$$

where the symbolic sequences between two delimiters | are the same as those in the model given in Ref. [16]. We have used them to examine possible orbits in the U sequence up to order 9. The results of symbolic sequences not greater than RLR are given in Table I. We see that the symbolic sequences RLR^4LRX, RLR^2LRLRX, RLR^2LRX, and RLR^2LR^3X are forbidden, i.e., there are no corresponding periodic orbits in the phase space.

TABLE I. Admissibility of the periodic sequences not greater than RLR and up to period 9 from the time series. Here X in a sequence stands for L or R. Only nonrepeating strings of the sequences are given. If the kth shift of the periodic sequence $P^\infty\bullet P^\infty$ is allowed or forbidden by a tangency T, we write the upper criterion as kT.

Sequence	Period	Admissibility	Upper criterion	Lower criterion
R	1	allowed	$0c_1$	$0c_4$
RL	2	allowed	$0c_11c_1$	$0c_31\bar{c}_3$
$RLRR$	4	allowed	$0c_21c_12c_13c_1$	$0c_31\bar{c}_32c_33\bar{c}_3$
$RLRRRLRL$	8	allowed	$0c_31c_12c_13c_14c_25c_16c_17c_1$	$0c_41\bar{c}_32c_33\bar{c}_34c_35\bar{c}_56c_37\bar{c}_3$
$RLRRRL$	6	undetermined		$0c_31\bar{c}_32c_23\bar{c}_24c_35\bar{c}_3$
$RLRRRR$	6	undetermined		$0c_31\bar{c}_32c_43\bar{c}_44c_25\bar{c}_2$
$RLRRRRRL$	8	allowed	$0c_31c_12c_13c_14c_15c_16c_17c_1$	$0c_41\bar{c}_42c_23\bar{c}_24c_35\bar{c}_36c_37\bar{c}_3$
$RLRRRRRR$	8	allowed	$0c_31c_12c_13c_14c_15c_16c_17c_1$	$0c_41\bar{c}_42c_43\bar{c}_44c_25\bar{c}_36c_37\bar{c}_3$
$RLRRRRRRR$	9	allowed	$0c_31c_12c_13c_14c_15c_16c_17c_18c_1$	$0c_51\bar{c}_52c_43\bar{c}_44c_25\bar{c}_26c_37\bar{c}_38c_4$
$RLRRRRRRL$	9	allowed	$0c_31c_12c_13c_14c_15c_16c_17c_18c_1$	$0c_41\bar{c}_42c_33\bar{c}_24c_45\bar{c}_36c_37\bar{c}_38c_4$
$RLRRRRR$	7	allowed	$0c_31c_12c_13c_14c_15c_16c_1$	$0c_51\bar{c}_52c_33\bar{c}_54c_25\bar{c}_26c_3$
$RLRRRRL$	7	allowed	$0c_31c_12c_13c_14c_15c_16c_1$	$0c_51\bar{c}_52c_33\bar{c}_34c_35\bar{c}_36c_3$
$RLRRRRLRX$	9	forbidden	$0c_2$	
$RLRRR$	5	allowed	$0c_31c_12c_13c_14c_1$	$1c_32c_23\bar{c}_54c_3$
$RLRRL$	5	undetermined		$0c_51\bar{c}_52c_23\bar{c}_24c_3$
$RLRRLRLRX$	9	forbidden	$0c_3$	
$RLRRLRX$	7	forbidden	$0c_3$	
$RLRRLRRRX$	9	forbidden	$0c_3$	
$RLRRLRRR$	8	allowed	$0c_51c_12c_13c_44c_15c_16c_17c_1$	$1c_32c_53\bar{c}_54c_27c_2$
$RLRRLRRL$	8	allowed	$0c_51c_12c_13c_44c_15c_16c_17c_1$	$2c_23\bar{c}_24c_35c_57c_2$
RLR	3	undetermined		$1c_2$

Moreover, we see that symbolic sequence RLR^2L, which is determined as being allowed, as given in Table III of Ref. [16], cannot be determined by the tangency points. It comes from the difference between symbolic sequences of the tangency points from the time series and those for the dynamical model. Thus symbolic dynamics from the time series can display the dynamical behavior of the model at the finite level of accuracy.

Consequently, we have determined grammatical rules and established symbolic dynamics from chaotic time series with a driven frequency. The symbolic dynamics is consistent with that of the model at a finite level of accuracy.

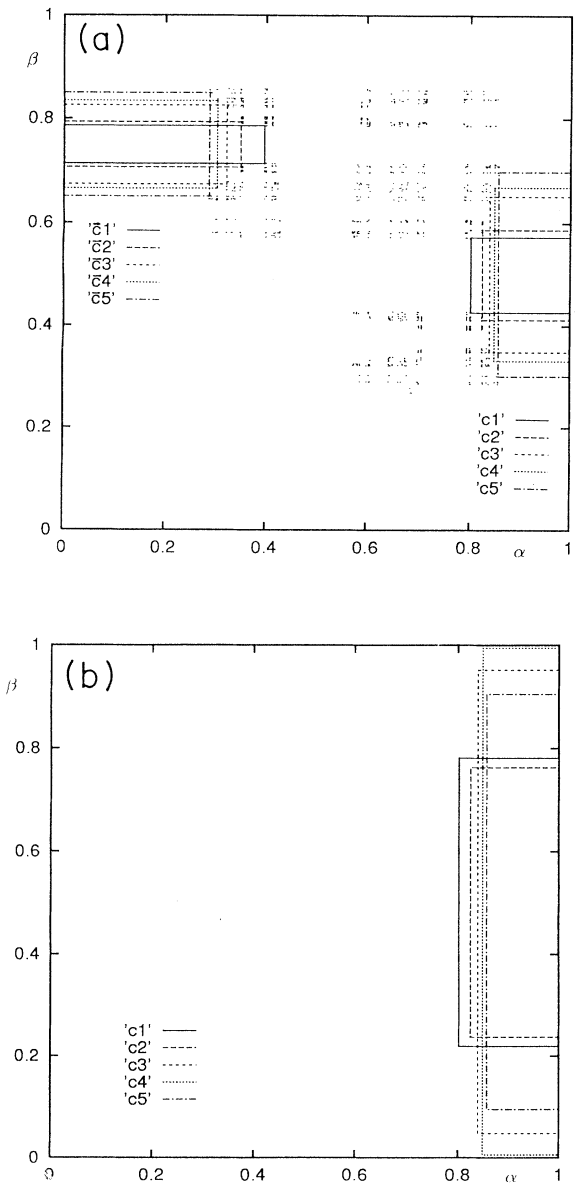

FIG. 3. (a) Fundamental and forward forbidden zones in the symbolic plane according to the ordering rules (3) and (4). The points representing real orbits generated from time series are also shown. (b) Fundamental forbidden zone in the symbolic plane according to the ordering rules (3) and (5).

III. APPLICATION OF SYMBOLIC DYNAMICS

A. Finding unstable periodic orbits

After the symbolic dynamics from the time series is established, we display the global systematics of periodic orbits within the strange attractor and find unstable periodic orbits. For convenience, we define the direction from c_1 to c_5 along the partition line $C\bullet$ as the lower reach direction and the opposite direction as the upper reach direction.

First, for each allowed symbolic sequence, we can determine two backward foliations, between which the periodic point encoded by the symbolic sequence exists. In Table I we give the upper criterion for each allowed symbolic sequence, i.e., the periodic point encoded by the symbolic sequence exists at the lower reach of the backward foliation passing through the tangency. We can also determine the lower criterion for the symbolic sequence, i.e., the periodic point encoded by the symbolic sequence exists at the upper reach of the backward foliation passing through the tangency. For the set of tangencies $\{c_i\}=\{Q_iC \bullet X_iP_i\}$, if the shift of a sequence $\cdots s_{k-2}s_{k-1} \bullet s_k s_{k+1} \cdots$ satisfies the condition that the backward sequence $\cdots s_{k-2}s_{k-1}\bullet$ is between $Q_iR\bullet$ and $Q_iL\bullet$ and at the same time $\bullet X_iP_i > \bullet s_k s_{k+1} \cdots$, then the point encoded by this shift exists at the upper reach of the backward foliation passing through the tangency c_i. In order to determine the lower criterion for all shifts of the allowed symbolic sequence, we need to develop the admissibility condition for the forward map $\bar{C}\bullet=X\bullet$ of the tangency point $C\bullet$. In the symbolic plane of Fig. 3(a), the forward forbidden zone consists of the forbidden rectangles. Each of them is enclosed by the lines $QRX\bullet$, $QLX\bullet$, $\bullet P$, and $\bullet L^\infty$. We consider the set of tangencies $\{\bar{c}_i\}= \{Q_iCX_i\bullet P_i\}$ for $i = 1, \ldots, 5$. A symbolic sequence $U \bullet V$ with $U\bullet$ between $Q_iRX_i\bullet$ and $Q_iLX_i\bullet$ and at the same time $\bullet V < \bullet P_i$ must be forbidden by the tangency $\bar{c}_i$. In the symbolic plane the sequence $U \bullet V$ corresponds to a point inside the forbidden zone of the tangency $\bar{c}_i$. If the shift of a sequence $\cdots s_{k-2}s_{k-1} \bullet s_k s_{k+1} \cdots$ satisfies the condition that the backward sequence $\cdots s_{k-2}s_{k-1}\bullet$ is not between $Q_iRX_i\bullet$ and $Q_iLX_i\bullet$ and at the same time $\bullet P_i < \bullet s_k s_{k+1} \cdots$, then this shift is not forbidden by the tangency $\bar{c}_i$. Owing to the property of well-ordered foliations, the shift must be not forbidden by any tangencies. Thus we may say that the shift is allowed according to the tangency. A necessary and sufficient condition for a sequence to become an allowed one is that all of its shifts are allowed according to the set of tangencies. Moreover, if the shift of a sequence $\cdots s_{k-2}s_{k-1} \bullet s_k s_{k+1} \cdots$ satisfies the condition that the backward sequence $\cdots s_{k-2}s_{k-1}\bullet$ is between $Q_iRX_i\bullet$ and $Q_iLX_i\bullet$ and at the same time $\bullet P_i < \bullet s_k s_{k+1} \cdots$, then the point encoded by this shifted symbolic sequence exists at the upper reach of the backward foliation passing through the tangency $\bar{c}_i$. Thus we

may say that the lower criterion of the shifted symbolic sequence is the tangency $\bar{c}_i$. The result of the lower criterion for all nonforbidden symbolic sequences is also shown in Table I. So, according to the upper and lower criteria, i.e., the upper and lower reach backward foliations, we can obtain a coarse-grained distribution of the periodic points. For example, the point of the symbolic sequence R exists between its upper reach backward foliation c_1 and lower reach backward foliation c_4.

Second, the ordering for the forward sequences coincides with the distribution of periodic points along the backward foliations. Thus, after the distribution of each allowed symbolic sequence between the backward foliations is obtained, we can determine further a local region for the periodic point encoded by the symbolic sequence in terms of the stable eigenvectors at another two periodic points near the backward foliations. The boundary of the local region consists of the stable eigenvectors, the backward foliations. For example, the symbolic sequences RLR^5L and RLR^4L exist between the symbolic sequences RLR^3L and RLR^2LR^2L according to the ordering rule for forward sequences. The points of $L\bullet RLR^5$ and $L\bullet RLR^4$ exist between the backward foliations passing through tangencies c_3 and c_5. Thus we can determine that the points of symbolic sequences $L \bullet RLR^5$ and $L \bullet RLR^4$ exist in a local region that consists of the stable eigenvectors at the periodic points encoded by $L \bullet RLR^3$ and $L \bullet RLR^2LR^2$, and backward foliations passing through tangencies c_3 and c_5, as shown in the region of part L of Fig. 2.

Third, the distribution of the forward and backward foliations in the strange attractor can be displayed approximately by that of the stable and unstable eigenvectors at each periodic point. For example, the symbolic sequence $R\bullet RLR^5$ exists between $R\bullet RLR^3$ and $R\bullet RLR^4$ according to the ordering rules for forward and backward sequences; this allows us to determine that the periodic point encoded by the symbolic sequence $R\bullet RLR^5$ exists in a square that consists of stable and unstable eigenvectors at the periodic points encoded by symbolic sequences $R\bullet RLR^3$ and $R\bullet RLR^4$, as shown in the region of part R of Fig. 2.

After the global systematics of periodic orbits within the strange attractor is obtained by establishing symbolic dynamics, we can apply symbolic dynamics to find different periodic orbits. From Table I, it is easy to know that the symbolic sequence $R\bullet RLR^6$ exists between the backward foliations c_3 and c_5 and in a square that consists of the stable and unstable eigenvectors at the periodic points encoded by $R\bullet RLR^5$ and $R\bullet RLR^4$. From the initial local square, we find the periodic orbit RLR^7 using the method of close returns. In the same way, we also find the periodic orbit RLR^6L. Therefore, we have displayed the global systematics of periodic orbits within the strange attractor and applied the symbolic dynamics to find unstable periodic orbits.

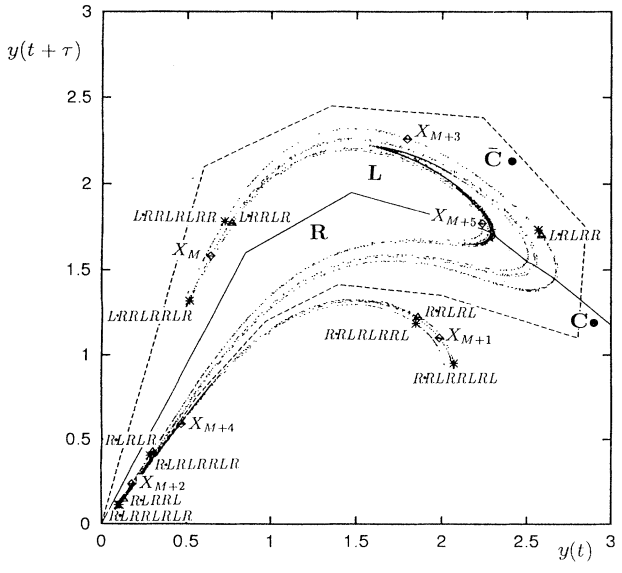

FIG. 4. Strange attractor with all points of two periodic orbits RLR^2L and RLR^2LR^2L and the last point X_M with five points of its forward orbit in the delay Poincaré section $[y(t), y(t+\tau); T/10]$.

B. Predicting chaotic time series and symbolic sequences

The strange attractor is referred to as the closure of the union of unstable periodic points. Each segment of a chaotic orbit can be approximated by a periodic orbit. After the global systematics of periodic orbits is found, we can draw the last reconstructed vector in the delay Poincaré section and find two nearest periodic points along a backward foliation near the vector. We can also determine that the two periodic orbits are close to the last segment of the chaotic orbit if some symbols of the backward sequence of the last vector is coincident with those of the two periodic orbits. Then, according to the two periodic orbits, we can predict a delay Poincaré map of the vector applying symbolic dynamics. For example, in Fig. 4 we take a segment of the reconstructed orbit from the time series and draw a point from it as the last vector in the delay Poincaré section $[y(t), y(t+\tau); \phi]$. The last point is marked by $\mathbf{X}_M = [y(t_M), y(t_M+\tau)]$ and its backward sequence is $\cdots R^2LR^4L\bullet$. The symbolic sequences of the two nearest periodic points near the backward foliation passing through the tangency c_2 are $L \bullet RRLR$ and $L \bullet RRLRRLR$, respectively. It is easy to see that there are two backward symbols RL in the periodic sequences that are coincident with those for the point $\mathbf{X}_M$. The delay Poincaré map $\mathbf{X}_{M+1} = [y(t_{M+1}), y(t_{M+1}+\tau)]$ of the last point exists between the periodic points encoded by symbolic sequences $R\bullet RLRL$ and $R \bullet RLRRLRL$ near the backward foliation passing through the tangency $\bar{c}_3$, i.e., a shift of $L \bullet RRLR$ and $L \bullet RRLRRLR$, respectively. The points for symbolic sequences $R \bullet RLRL$ and $R \bullet RLRRLRL$ are at

(1.86,1.22) and (2.07,0.95), respectively. Thus we obtain a local region of predicted point $\mathbf{X_{M+1}}$ and estimate that its horizontal and vertical values are $1.86 < y(t_{M+1}) < 2.07$ and $0.95 < y(t_{M+1}+\tau) < 1.22$, respectively. In the same way, the points for symbolic sequences $R \bullet LRLR$ and $R \bullet LRRLRLR$ are at (0.30,0.43) and (0.10,0.11), respectively. Thus the coordinates of predicted point $\mathbf{X}_{M+2} = [y(t_{M+2}), y(t_{M+2}+\tau)]$ are estimated as $0.10 < y(t_{M+2}) < 0.30$ and $0.11 < y(t_{M+2}+\tau) < 0.43$. Further, again and again, we can predict more delay Poincaré maps and approximately estimate their values. In Fig. 4 we also draw five exact points in the forward orbit of the last point $\mathbf{X}_M$. According to a comparison between the exact and estimated values, we can determine that the method of prediction is effective. Moreover, since there is an instability in the strange attractor, the more delay Poincaré maps there are, the worse accuracy the predicted values have. But we find that the predicted symbolic sequence $RRLR$ agrees with the forward sequence of two periodic points encoded by $L \bullet RRLR$ and $L \bullet RRLRRLR$. Thus we can obtain a predicted symbolic sequence with high accuracy at the finite steps. Moreover, when the initial phase ϕ is changed in a period T, we can predict a chaotic orbit with finite accuracy and its symbolic sequence with high accuracy. Therefore, we have applied the symbolic dynamics to predict the time series with finite accuracy as well as symbolic sequences with high accuracy.

IV. SUMMARY AND CONCLUSION

A simple method to determine a partition line from chaotic time series with a driven frequency has been devised, so that the embedded strange attractor can be divided effectively by the partition line. After the determination of grammatical rules, symbolic dynamics has been established from the chaotic time series. The symbolic dynamics provides a global systematics of unstable periodic orbits within the strange attractor. With the global property, the symbolic dynamics has been applied to find unstable periodic orbits and predict the chaotic time series with finite accuracy and symbolic sequences with high accuracy.

ACKNOWLEDGMENTS

The author thanks Professor B.-L. Hao and Professor W.-M. Zheng for their encouragement. This work was supported partially by the National Natural Science Foundation of China.

[1] E. N. Lorenz, J. Atmos. Sci. **20**, 130 (1963).
[2] R. H. Simoyi, A. Wolf, and H. L. Swinney, Phys. Rev. Lett. **49**, 245 (1982).
[3] F. T. Arecchi, R. Meucci, G. P. Puccioni, and J. R. Tredicce, Phys. Rev. Lett. **49**, 1217 (1982).
[4] P. Boesiger, E. Brun, and D. Meier, Phys. Rev. Lett. **38**, 602 (1977).
[5] N. H. Packard, J. P. Crutchfield, J. D. Farmer, and R. S. Shaw, Phys. Rev. Lett. **45**, 712 (1980).
[6] F. Takens, in *Dynamical Systems and Turbulence*, edited by D. A. Rand and L.-S. Young, Lecture Notes in Mathematics Vol. 898 (Springer-Verlag, Berlin, 1981).
[7] T. Sauer, J. A. Yorke, and M. Casdagli, J. Stat. Phys. **65**, 579 (1991).
[8] J.-P. Eckmann and D. Ruelle, Rev. Mod. Phys. **57**, 617 (1985).
[9] B.-L. Hao, Physica D **51**, 161 (1991).
[10] P. Cvitanovic, G. H. Gunaratne, and I. Procaccia, Phys. Rev. **38A**, 1503 (1988).
[11] H. Zhao and W.-M. Zheng, Commun. Theor. Phys. **19**, 21 (1993).
[12] H. G. Solari and R. Gilmore, Phys. Rev. A **37**, 3096 (1988); **38**, 1566 (1988).
[13] G. B. Mindlin, H. G. Solari, M. A. Natiello, R. Gilmore, and X.-J. Hou, J. Nonlin. Sci. **1**, 147 (1991).
[14] L. Flepp, R. Holzner, E. Brun, M. Finardi, and R. Badii, Phys. Rev. Lett. **67**, 2244 (1991).
[15] J.-X. Liu, Z.-B. Wu, and W.-M. Zheng, Commun. Theor. Phys. (to be published).
[16] Z.-B. Wu, Phys. Rev. E (to be published).
[17] D. P. Lathrop and E. J. Kostelich, Phys. Rev. A **40**, 4028 (1989).
[18] B.-L. Hao, *Elementary Symbolic Dynamics and Chaos in Dissipative Systems* (World Scientific, Singapore, 1989).
[19] J.-P. Eckmann, S. O. Kamphorst, D. Ruelle, and S. Ciliberto, Phys. Rev. A **34**, 4971 (1986).
[20] J. M. Greene, in *Long-Time Prediction in Dynamics*, edited by C. W. Horton, J. L. E. Reichl, and V. G. Szebehely (Wiley, New York, 1983).
[21] Y. Gu, Phys. Lett. A **124**, 340 (1987).